Progress In Electromagnetics Research, PIER 81, 315–328, 2008

ROBUST ADAPTIVE BEAMFORMING FOR A CLASS OF GAUSSIAN STEERING VECTOR MISMATCH

Y. J. Gu, Z. G. Shi, and K. S. Chen

Department of Information and Electronic Engineering
Zhejiang University
Hangzhou 310027, China

Y. Li

Department of Communication and Electronic Engineering
East China University of Science and Technology
Shanghai 200237, China

Abstract—Compared with the worst-case optimization-based approach, the probability-constrained approach is a more flexible one to robust adaptive beamforming. In this paper, a precise relationship between the two approaches is built in the case of Gaussian steering vector mismatch, which shows that the probability-constrained beamformer design can be interpreted in terms of the worst-case beamformer design. Numerical simulations demonstrate that the precise version of the probability-constrained beamformer is more robust to the steering vector mismatch than the other popular robust adaptive beamformers.

1. INTRODUCTION

Compared with the traditional data-independent beamformers, the adaptive beamformers can have better resolution and much better interference rejection capability [1–3]. In the past decades, adaptive beamforming has been widely used in radar [4, 5], direction finding (DF) [6–8], wireless communications [9], medical imaging [10], and other areas [11, 12]. However, the adaptive beamformers are much more sensitive to the steering vector errors, which will degrade the performance of the adaptive beamformers severely [13, 14]. Therefore, the robustness against the steering vector uncertainties in adaptive beamformers is required [15–17].

As a recent popular approach to designing robust adaptive beamformer, the worst-case optimization-based robust adaptive beamforming [8–10] makes explicit use of an uncertainty set of the array steering vector, which is unlike the early robust beamforming methods. The worst-case robust beamformers are designed to minimize the output interference-plus-noise power, while maintain distortionless response for all possible steering vectors which belong to the uncertainty set. However, the actual worst conditions may occur in practice with a rather low probability, and so, the worst-case robust beamforming may be overly conservative in practical applications.

In order to overcome the conservative character of the worst-case robust beamforming, a probability-constrained robust adaptive beamforming was proposed in [11, 12], which is more flexible than the former. The probability-constrained robust adaptive beamforming is to maintain the beamformer distortionless response only for those operational conditions with a sufficiently high probability, rather than for all operational conditions corresponding to the uncertainty set. In the case of Gaussian steering vector mismatch, the worst-case robust beamformer can be viewed as a strengthened version of the probability-constrained robust beamformer in [12]. However, [12] didn't reveal the real relationship between the two robust adaptive beamforming approaches. In this paper, we build a precise relationship between the two robust beamforming approaches in the case of Gaussian steering vector mismatch. Simulation results confirm that compared with the previous robust adaptive beamforming approaches, the precise version of the probability-constrained robust beamformer is more robust.

The rest of this paper is organized as follows. Section 2 contains background material. In Section 3, we formulate a precise relationship between the worst-case optimization-based and probability-constrained approaches to robust adaptive beamforming for a class of Gaussian steering vector mismatch. The performance comparisons are presented in 4. Finally, Section 5 concludes this paper.

2. BACKGROUND

The output of a narrowband beamformer is given by

$$y(k) = \boldsymbol{\omega}^H \mathbf{x}(k), \tag{1}$$

where k is the time index, $\mathbf{x}(k) = [x_1(k), \cdots, x_N(k)]^T \in \mathcal{C}^{N\times 1}$ is the complex vector of array observations, $\boldsymbol{\omega} = [\omega_1, \cdots, \omega_N]^T \in \mathcal{C}^{N\times 1}$ is the complex vector of beamformer weights, N is the number of array sensors, and $(\cdot)^T$ and $(\cdot)^H$ denote the transpose and Hermitian

transpose, respectively. The observation vector has the form

$$\mathbf{x}(k) = \mathbf{a}s(k) + \boldsymbol{i}(k) + \boldsymbol{n}(k), \quad k = 1, 2, \cdots \tag{2}$$

where $\mathbf{a}$ is the signal steering vector, $s(k)$, $\boldsymbol{i}(k)$, and $\boldsymbol{n}(k)$ are the desired signal, interference and noise components, respectively. The source, interference and noise are assumed to be zero-mean, complex Gaussian white processes that are statistically independent. The weight vector $\boldsymbol{\omega}$ is chosen to maximize the array output signal-to-interference-plus-noise ratio (SINR)

$$SINR = \frac{\sigma_s^2 |\boldsymbol{\omega}^H \mathbf{a}|^2}{\boldsymbol{\omega}^H \mathbf{R}_{\mathbf{i+n}} \boldsymbol{\omega}}, \tag{3}$$

where $\sigma_s^2 = E\{|s(k)|^2\}$ is the signal power, and $\mathbf{R}_{i+n} = E\{(\mathbf{i}(k) + \mathbf{n}(k))(\mathbf{i}(k) + \mathbf{n}(k))^H\}$ is the $N \times N$ interference-plus-noise covariance matrix. Here, $E\{\cdot\}$ denotes the statistical mean. In practical applications, the exact $\mathbf{R}_{\mathbf{i+n}}$ is unavailable, and it is usually replaced by the sample covariance matrix [13]

$$\hat{\mathbf{R}} = \frac{1}{K} \sum_{k=1}^{K} \mathbf{x}(k)\mathbf{x}(k)^H, \tag{4}$$

where K is the number of snapshots.

The classical Capon method is to maintain a distortionless response toward the desired signal and minimize the output interference-plus-noise power [14]. Hence, the problem of maximizing the SINR in (3) can be written as the following optimization problem

$$\min_{\boldsymbol{\omega}} \ \boldsymbol{\omega}^H \hat{\mathbf{R}} \boldsymbol{\omega} \quad s.t. \quad \boldsymbol{\omega}^H \mathbf{a} = 1, \tag{5}$$

which can be solved by the Lagrange multiplier method and the solution

$$\boldsymbol{\omega}_{MV} = \frac{\hat{\mathbf{R}}^{-1}\mathbf{a}}{\mathbf{a}^H \hat{\mathbf{R}}^{-1}\mathbf{a}} \tag{6}$$

is referred to as the sample matrix inversion (SMI) minimum variance distortionless response (MVDR) beamformer.

However, the SMI MVDR beamformer (6) has an essential shortcoming that it does not provide sufficient robustness against the mismatch between the presumed and actual signal steering vectors, which degrades the beamformer performance severely. In the recent

popular worst-case robust adaptive beamforming, the actual steering vector $\bar{\mathbf{a}}$ is modeled as additive uncertainty, namely,

$$\bar{\mathbf{a}} = \mathbf{a} + \boldsymbol{\delta}, \tag{7}$$

where $\mathbf{a}$ is the presumed steering vector, and $\boldsymbol{\delta}$ denotes the steering vector mismatch. In the design of the worst-case robust beamformer, the norm of the steering vector mismatch is assumed to have an upper bound $\varepsilon > 0$, namely, $\| \boldsymbol{\delta} \| \leq \varepsilon$. The design of the worst-case robust adaptive beamformer can be expressed as the following optimization problem [8]:

$$\min_{\boldsymbol{\omega}} \ \boldsymbol{\omega}^H \hat{\mathbf{R}} \boldsymbol{\omega} \quad s.t. \quad \min_{\|\boldsymbol{\delta}\| \leq \varepsilon} |\boldsymbol{\omega}^H (\mathbf{a} + \boldsymbol{\delta})| \geq 1. \tag{8}$$

As [8–10] denote, the worst-case robust beamformer (8) belongs to the class of diagonal loading technologies. Unlike the diagonal loading sample matrix inversion (DL-SMI) beamformer [15], the diagonal loading factor of the worst-case robust beamformer can be precisely calculated [9].

However, the worst-case robust beamforming (8) may be overly conservative, because the actual worst operational conditions may occur in practice with a very low probability. In [11, 12], a more flexible approach to the robust adaptive beamformer design was proposed, which maintains the beamformer distortionless response only for those operational conditions with a sufficiently high probability rather than for all possible steering vector. The probability-constrained robust adaptive beamforming can be formulated as the following optimization problem:

$$\min_{\boldsymbol{\omega}} \ \boldsymbol{\omega}^H \hat{\mathbf{R}} \boldsymbol{\omega} \qquad s.t. \ \ Pr\{|\boldsymbol{\omega}^H (\mathbf{a} + \boldsymbol{\delta})| \geq 1\} \geq p, \tag{9}$$

where $Pr\{\cdot\}$ stands for the probability operator, and p is a preselected probability value that is related to the beamformer outage probability p_{out} with $p = 1 - p_{out}$.

When the distribution of $\boldsymbol{\delta}$ is unknown, the probability-constrained robust beamformer degrades into the worst-case robust beamformer [12]. In this paper, we focus on the Gaussian steering vector mismatch $\boldsymbol{\delta}$ with zero mean and covariance matrix $\mathbf{C}_{\boldsymbol{\delta}}$, that is,

$$\boldsymbol{\delta} \sim \mathcal{CN}(\mathbf{0}_N, \mathbf{C}_{\boldsymbol{\delta}}), \tag{10}$$

where $\mathbf{0}_N$ is an $N \times 1$ zero vector. The covariance matrix $\mathbf{C}_{\boldsymbol{\delta}}$ captures the second-order statistics of the uncertainties in the steering vector. Even though $\mathbf{C}_{\boldsymbol{\delta}}$ is actually non-diagonal, it typically can be approximated by the scaled identity matrix for the simplicity reason [16].

3. PROBABILITY-CONSTRAINED ROBUST MINIMUM VARIANCE BEAMFORMING

Using the assumption (10), it is easy to show that the random variable $\boldsymbol{\omega}^H(\mathbf{a}+\boldsymbol{\delta})$ has the following distribution

$$\boldsymbol{\omega}^H(\mathbf{a}+\boldsymbol{\delta}) \sim \mathcal{CN}\left(\boldsymbol{\omega}^H\mathbf{a}, \parallel \mathbf{C}_{\boldsymbol{\delta}}^{1/2}\boldsymbol{\omega} \parallel^2\right), \tag{11}$$

and its real and imaginary parts $\Re\{\boldsymbol{\omega}^H(\mathbf{a}+\boldsymbol{\delta})\}$ and $\Im\{\boldsymbol{\omega}^H(\mathbf{a}+\boldsymbol{\delta})\}$ are real Gaussian i.i.d., that is,

$$\begin{aligned} \Re\{\boldsymbol{\omega}^H(\mathbf{a}+\boldsymbol{\delta})\} &\sim \mathcal{N}\left(\Re\{\boldsymbol{\omega}^H\mathbf{a}\}, \parallel \mathbf{C}_{\boldsymbol{\delta}}^{1/2}\boldsymbol{\omega} \parallel^2 /2\right) \\ \Im\{\boldsymbol{\omega}^H(\mathbf{a}+\boldsymbol{\delta})\} &\sim \mathcal{N}\left(\Im\{\boldsymbol{\omega}^H\mathbf{a}\}, \parallel \mathbf{C}_{\boldsymbol{\delta}}^{1/2}\boldsymbol{\omega} \parallel^2 /2\right). \end{aligned} \tag{12}$$

Hence, the random variable $|\boldsymbol{\omega}^H(\mathbf{a}+\boldsymbol{\delta})| = \sqrt{\begin{matrix}\Re\{\boldsymbol{\omega}^H(\mathbf{a}+\boldsymbol{\delta})\}^2+ \\ \Im\{\boldsymbol{\omega}^H(\mathbf{a}+\boldsymbol{\delta})\}^2\end{matrix}}$ has a Ricean distribution. From [17], the probability constraint in (9) can be simplified as

$$\begin{aligned} &Pr\left\{|\boldsymbol{\omega}^H(\mathbf{a}+\boldsymbol{\delta})| \geq 1\right\} \\ &\quad \approx 1 - Pr\left\{|\boldsymbol{\omega}^H(\mathbf{a}+\boldsymbol{\delta})| \leq 1\right\} \\ &\quad = e^{-(|\boldsymbol{\omega}^H\mathbf{a}|^2+1)/\|\mathbf{C}_{\boldsymbol{\delta}}^{1/2}\boldsymbol{\omega}\|^2} \sum_{k=0}^{\infty} |\boldsymbol{\omega}^H\mathbf{a}|^k I_k\left(\frac{2|\boldsymbol{\omega}^H\mathbf{a}|}{\parallel \mathbf{C}_{\boldsymbol{\delta}}^{1/2}\boldsymbol{\omega} \parallel}\right) \geq p, \end{aligned} \tag{13}$$

where $I_\alpha(x)$ is the αth-order modified Bessel function of the first kind, which can be represented by infinite series

$$I_\alpha(x) = \sum_{k=0}^{\infty} \frac{(x/2)^{\alpha+2k}}{k!\Gamma(\alpha+k+1)}, \qquad x \geq 0. \tag{14}$$

Then, the probability-constrained optimization problem (9) is equivalent to the following determined constrained optimization problem:

$$\min_{\boldsymbol{\omega}} \boldsymbol{\omega}^H\hat{\mathbf{R}}\boldsymbol{\omega} \;\; s.t. \;\; e^{-(|\boldsymbol{\omega}^H\mathbf{a}|^2+1)/\|\mathbf{C}_{\boldsymbol{\delta}}^{1/2}\boldsymbol{\omega}\|^2} \sum_{k=0}^{\infty} |\boldsymbol{\omega}^H\mathbf{a}|^k I_k\left(\frac{2|\boldsymbol{\omega}^H\mathbf{a}|}{\parallel \mathbf{C}_{\boldsymbol{\delta}}^{1/2}\boldsymbol{\omega} \parallel}\right) \geq p, \tag{15}$$

which is almost an insoluble problem without effective simplification. In the following, we will approximate the probability constraint in (9) into a simple determined constraint.

Let us assume that the steering vector errors are not too large, so that $|\boldsymbol{\omega}^H\boldsymbol{\delta}| < |\boldsymbol{\omega}^H\mathbf{a}|$ is valid. Applying the triangle inequality, we have

$$|\boldsymbol{\omega}^H(\mathbf{a}+\boldsymbol{\delta})| \geq |\boldsymbol{\omega}^H\mathbf{a}| - |\boldsymbol{\omega}^H\boldsymbol{\delta}|. \tag{16}$$

Moreover, it is easy to verify that

$$|\boldsymbol{\omega}^H(\mathbf{a}+\boldsymbol{\delta})| = |\boldsymbol{\omega}^H\mathbf{a}| - |\boldsymbol{\omega}^H\boldsymbol{\delta}| \tag{17}$$

if

$$\angle\{\boldsymbol{\omega}^H\boldsymbol{\delta}\} = -\angle\{\boldsymbol{\omega}^H\mathbf{a}\}. \tag{18}$$

From (16), it follows that

$$Pr\{|\boldsymbol{\omega}^H(\mathbf{a}+\boldsymbol{\delta})| \geq 1\} \geq Pr\{|\boldsymbol{\omega}^H\mathbf{a}| - |\boldsymbol{\omega}^H\boldsymbol{\delta}| \geq 1\}, \tag{19}$$

which can be used to approximate the constraint in (9). Indeed, according to (19), the probability constraint in (9) is always satisfied if

$$Pr\{|\boldsymbol{\omega}^H\mathbf{a}| - |\boldsymbol{\omega}^H\boldsymbol{\delta}| \geq 1\} \geq p. \tag{20}$$

With the character that the object function $\boldsymbol{\omega}^H\hat{\mathbf{R}}\boldsymbol{\omega}$ is rotation-invariant to $\boldsymbol{\omega}$ [8], we can always rotate the phase of $\boldsymbol{\omega}$ so that $\boldsymbol{\omega}^H\mathbf{a}$ is a non-negative number, namely,

$$\Re\{\boldsymbol{\omega}^H\mathbf{a}\} \geq 0, \quad \Im\{\boldsymbol{\omega}^H\mathbf{a}\} = 0. \tag{21}$$

Then, the probability constraint (20) can be rewritten as

$$Pr\{|\boldsymbol{\omega}^H\boldsymbol{\delta}| \leq \boldsymbol{\omega}^H\mathbf{a} - 1\} \geq p. \tag{22}$$

In [12], the probability constraint (20) was replaced by the following strengthened constraint:

$$Pr\{|\Re\{\boldsymbol{\omega}^H\boldsymbol{\delta}\}| \leq (\boldsymbol{\omega}^H\mathbf{a}-1)/\sqrt{2},\ |\Im\{\boldsymbol{\omega}^H\boldsymbol{\delta}\}| \leq (\boldsymbol{\omega}^H\mathbf{a}-1)/\sqrt{2}\} \geq p \tag{23}$$

from the character that

$$\begin{aligned} &Pr\{|\Re\{\boldsymbol{\omega}^H\boldsymbol{\delta}\}| \leq (\boldsymbol{\omega}^H\mathbf{a}-1)/\sqrt{2}, |\Im\{\boldsymbol{\omega}^H\boldsymbol{\delta}\}| \leq (\boldsymbol{\omega}^H\mathbf{a}-1)/\sqrt{2}\} \\ &\leq Pr\{|\boldsymbol{\omega}^H\boldsymbol{\delta}| \leq \boldsymbol{\omega}^H\mathbf{a}-1\}. \end{aligned} \tag{24}$$

Using (10), the strengthened version of the probability-constrained problem (9) can be expressed as the determined constrained optimization problem [12]

$$\min_{\boldsymbol{\omega}}\ \boldsymbol{\omega}^H\hat{\mathbf{R}}\boldsymbol{\omega} \quad s.t. \quad \sqrt{2}\ erf^{-1}(\sqrt{p})\ \|\ \mathbf{C}_{\boldsymbol{\delta}}^{1/2}\boldsymbol{\omega}\ \| \leq \boldsymbol{\omega}^H\mathbf{a} - 1, \tag{25}$$

where $erf^{-1}(z)$ denotes the inverse function of the normalized error function for the Gaussian distribution

$$erf(z) = \frac{2}{\sqrt{\pi}} \int_0^z e^{-x^2} dx. \tag{26}$$

As [12] denotes, the optimization problem (25) can be identified to the second-order cone programming (SOCP) problem which is exactly equivalent to the worst-case robust adaptive beamforming problem of [8] provided that $\mathbf{C}_{\boldsymbol{\delta}} = \sigma_{\boldsymbol{\delta}}^2 \mathbf{I}$ and

$$\varepsilon_s = \sigma_{\boldsymbol{\delta}} \sqrt{2}\ erf^{-1}(\sqrt{p}) = \sigma_{\boldsymbol{\delta}} \sqrt{2}\ erf^{-1}(\sqrt{1 - p_{out}}). \tag{27}$$

The performance of the probability-constrained robust adaptive beamformer just depends on ε_s, which is the sole parameter of the equivalent worst-case optimization problem.

However, the Equation (27) doesn't reveal the real relationship between the two approaches to robust adaptive beamforming because of introducing the constraint (23). In the following, we will reveal the precise relationship between the two approaches without any additional simplification. From (10), the random variable $\boldsymbol{\omega}^H \boldsymbol{\delta}$ has the following distribution

$$\boldsymbol{\omega}^H \boldsymbol{\delta} \sim \mathcal{CN}(0, \parallel \mathbf{C}_{\boldsymbol{\delta}}^{1/2} \boldsymbol{\omega} \parallel^2), \tag{28}$$

and its real and imaginary parts $\Re\{\boldsymbol{\omega}^H \boldsymbol{\delta}\}$ and $\Im\{\boldsymbol{\omega}^H \boldsymbol{\delta}\}$ are real Gaussian i.i.d., that is,

$$\begin{aligned} \Re\{\boldsymbol{\omega}^H \boldsymbol{\delta}\} &\sim \mathcal{N}\left(0, \parallel \mathbf{C}_{\boldsymbol{\delta}}^{1/2} \boldsymbol{\omega} \parallel^2 /2\right) \\ \Im\{\boldsymbol{\omega}^H \boldsymbol{\delta}\} &\sim \mathcal{N}\left(0, \parallel \mathbf{C}_{\boldsymbol{\delta}}^{1/2} \boldsymbol{\omega} \parallel^2 /2\right). \end{aligned} \tag{29}$$

Then, the random variable $|\boldsymbol{\omega}^H \boldsymbol{\delta}| = \sqrt{\Re\{\boldsymbol{\omega}^H \boldsymbol{\delta}\}^2 + \Im\{\boldsymbol{\omega}^H \boldsymbol{\delta}\}^2}$ has a Rayleigh density. From [18], we can simplify the probability constraint (22) as the equivalent deterministic form

$$Pr\left\{|\boldsymbol{\omega}^H \boldsymbol{\delta}| \leq \boldsymbol{\omega}^H \mathbf{a} - 1\right\} = 1 - e^{-(\boldsymbol{\omega}^H \mathbf{a} - 1)^2 / (\|\mathbf{C}_{\boldsymbol{\delta}}^{1/2} \boldsymbol{\omega}\|^2)} \geq p, \tag{30}$$

or, equivalently,

$$\sqrt{\ln\left(\frac{1}{1-p}\right)} \parallel \mathbf{C}_{\boldsymbol{\delta}}^{1/2} \boldsymbol{\omega} \parallel \leq \boldsymbol{\omega}^H \mathbf{a} - 1. \tag{31}$$

Hence, the probability-constrained optimization problem (9) can be expressed as

$$\min_{\boldsymbol{\omega}} \ \boldsymbol{\omega}^H \hat{\mathbf{R}} \boldsymbol{\omega} \quad s.t. \quad \sqrt{\ln\left(\frac{1}{1-p}\right)} \parallel \mathbf{C}_{\boldsymbol{\delta}}^{1/2} \boldsymbol{\omega} \parallel \leq \boldsymbol{\omega}^H \mathbf{a} - 1, \tag{32}$$

which can be identified as a SOCP problem [19] and is exactly equivalent to the worst-case robust adaptive beamforming problem of [8] provided that $\mathbf{C}_{\boldsymbol{\delta}} = \sigma_{\boldsymbol{\delta}}^2 \mathbf{I}$ and

$$\varepsilon = \sigma_{\boldsymbol{\delta}} \sqrt{\ln\left(\frac{1}{1-p}\right)} = \sigma_{\boldsymbol{\delta}} \sqrt{\ln\left(\frac{1}{p_{out}}\right)}. \tag{33}$$

In summary, in the case of Gaussian steering vector mismatch, the probability-constrained robust beamformer (9) can be simplified as the worst-case robust beamformer (32), and the Equation (33) explicitly quantifies the relationship between the two approaches providing an interpretation of the worst-case design parameter ε in terms of the beamformer outage probability p_{out}.

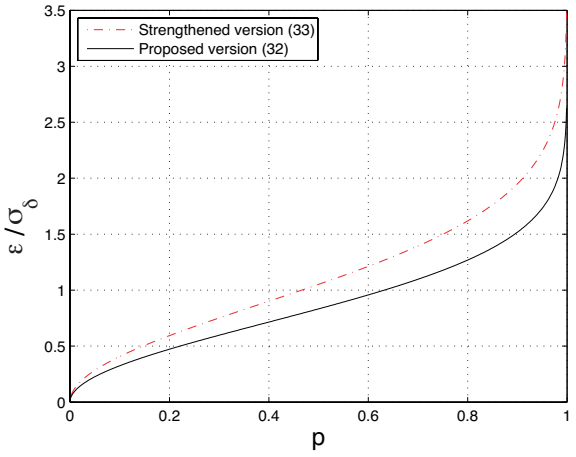

Figure 1. Equivalent radius vs. probability p.

Comparing (33) with (27), for the same preselected probability p, we can observe that the radius of the spherical uncertainty region suggested by the equivalent SOCP problem of the strengthened version (25) is larger than that of the precise version (32), namely,

$$\varepsilon_s \geq \varepsilon, \tag{34}$$

which is shown in Figure 1. Note that ε in (33) is a monotonically increasing function of $p \in [0, 1)$. From (34), we can see that the strengthened version (25) is in fact with a larger probability than the preselected one, which is caused by strengthening the probability constraint (22) by (23).

In the following section, we will compare the performance of the precise version of the probability-constrained robust beamformer with some other methods through numerical simulations.

4. PERFORMANCE COMPARISON

In our simulations, a uniform linear array (ULA) with $N = 10$ omnidirectional sensors spaced half a wavelength apart is considered. Without loss of generality, we assume that there are two interfering sources with plane wavefronts and the directions of arrival (DOAs) equal to 30° and 50°, respectively. A total of 200 Monte Carlo simulation runs are used to obtain each simulated point. Four different beamforming algorithms are compared in terms of the mean output SINR: the precise version (32) of the probability-constrained robust beamformer, the strengthened version (25) of the probability-constrained robust beamformer, the eigenspace-based beamformer [20], and the worst-case robust beamformer [8] with $\varepsilon = 3$ (as a good *ad hoc* choice of this parameter recommended in [8]). As a reference, the optimal output SINR

$$SINR_{opt} = \sigma_s^2 \mathbf{a}^H \mathbf{R}_{\mathbf{i+n}}^{-1} \mathbf{a} \tag{35}$$

is also shown in all figures, which is obtained in the case of signal-free training samples [13].

A scenario with the Ricean propagation medium is considered where the presumed signal steering vector is a plane wave with the nominal DOA θ_0 while the actual steering vector corresponds to a spatially spread with the central angle θ_0. The actual mismatch vector $\boldsymbol{\delta}$ is modeled as [8]

$$\boldsymbol{\delta} = \frac{\sigma_\delta}{\sqrt{L}} \sum_{l=1}^{L} e^{j\psi_l} \mathbf{a}(\theta_0 + \theta_l), \tag{36}$$

where, σ_δ^2 characterizes the power of scattered nonline-of-sight (NLOS) signal components, L is their number, ψ_l is the phase shift parameter of the lth NLOS component, and θ_l is the angular shift of the lth NLOS component with respect to the nominal DOA. The parameters θ_l are assumed to be independently drawn in each simulation run from

a uniform random generator with zero mean and standard deviation $\sigma_\theta = 5°$. The parameters ψ_l are independently and uniformly drawn from the interval $[0, 2\pi)$ in each run. In all simulations, $L = 20$, $\theta_0 = 3°$ and $K = 50$ are taken and the covariance matrix $\mathcal{C}_{\boldsymbol{\delta}}$ is approximated by $\sigma_{\boldsymbol{\delta}}^2\mathbf{I}$.

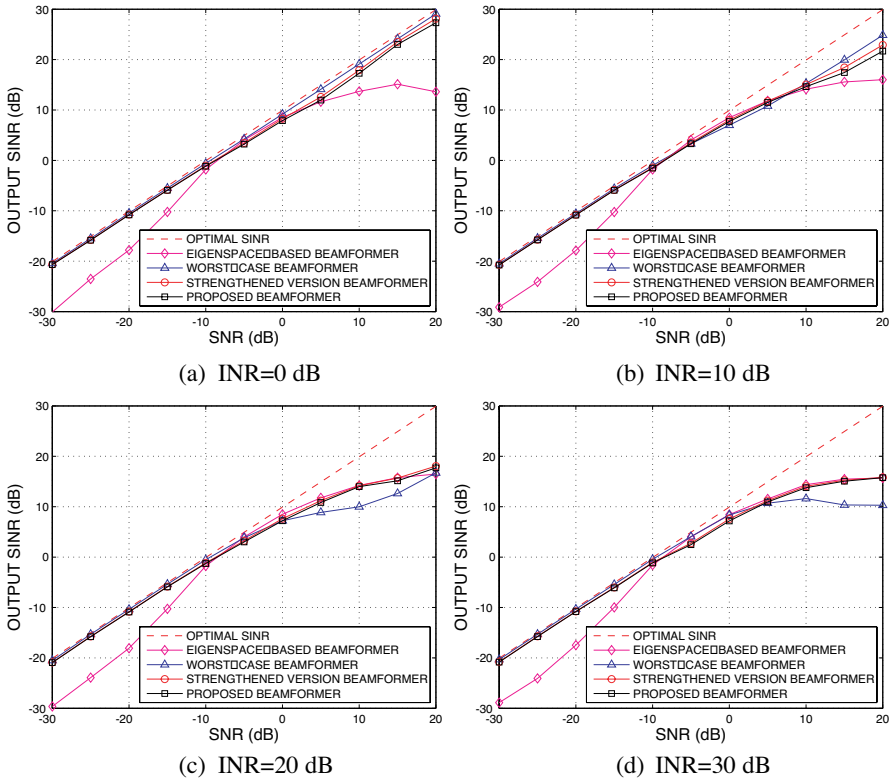

(a) INR=0 dB (b) INR=10 dB

(c) INR=20 dB (d) INR=30 dB

Figure 2. Output SINR versus SNR on different INR conditions, $p = 0.9$, $\sigma_{\boldsymbol{\delta}} = 0.3$.

In Figure 2, we compare the performances of different beamforming algorithms in terms of the mean output array SINR versus the input SNR on the different interference-to-noise ratio (INR) conditions for the typical probability $p = 0.9$ and $\sigma_{\boldsymbol{\delta}} = 0.3$. From Figure 2, we observe that when the variance of the element of the steering vector is relatively small, the two probability-constrained robust beamformers have obvious performance advantage over the worst-case robust beamformer at high INR. However, they perform not as well as the worst-case robust beamformer at low INR. In addition,

the strengthened version (25) has a slight performance advantage over the precise one (32), because the strengthen version has a relative larger radius.

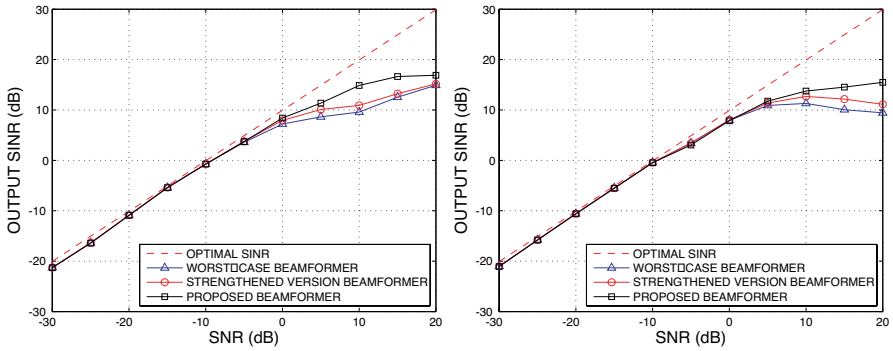

(a) INR=20 dB (b) INR=30 dB

Figure 3. Output SINR versus SNR on different INR conditions, $p = 0.9$, $\sigma_{\boldsymbol{\delta}} = 1.5$.

When $\sigma_{\boldsymbol{\delta}}$ is regarded as the variable of the radius function, we can observe that the slope of the radius ε_s (27) is larger than that of the radius ε (33) for any preselected probability p, which can also be seen from Figure 1. And then, the radius ε_s of the strengthened version increase faster than the radius ε of the precise version as the increase of $\sigma_{\boldsymbol{\delta}}$. In Figure 3, we compare the performances of two versions of probability-constrained beamforming algorithms in the case of $\sigma_{\boldsymbol{\delta}} = 1.5$, which is 5 times of $\sigma_{\boldsymbol{\delta}} = 0.3$ in the simulations of Figure 2. The simulation results demonstrate that in the condition of large variance, the precise version (32) proposed in this paper keeps the good performance as well as in the condition of small variance, whereas the strengthened version (25) suffers the performance degradation at high SNR. In this sense, conclusion can be drawn that the precise version (32) is more robust than the other methods.

5. CONCLUSION

Compared with the worst-case optimization-based robust adaptive beamforming, the probability-constrained robust adaptive beamforming is a more flexible approach. In this paper, we build a precise relationship between the two approaches in the case of Gaussian steering vector mismatch. Simulation results demonstrate that the precise version of the probability-constrained beamformer is more robust to

the steering vector mismatch than the other popular robust adaptive beamformers.

ACKNOWLEDGMENT

This work was supported by Natural Science Foundation of China (No. 60531020, No. 60604029), Natural Science Foundation of Zhejiang Province (No. Y106384) and China Post Doctoral Science Foundation (No. 20060400313).

REFERENCES

1. Dessouky, M., H. Sharshar, and Y. Albagory, "Improving the cellular coverage from a high altitude platform by novel tapered beamforming technique," *Journal of Electromagnetic Waves and Applications*, Vol. 21, No. 13, 1721–1731, 2007.
2. Gu, Y. J., et al., "Robust adaptive beamforming for steering vector uncertainties based on equivalent DOAs method," *Progress In Electromagnetics Research*, PIER 79, 277–290, 2008.
3. Dessouky, M., H. Sharshar, and Y. Albagory, "A novel tapered beamforming window for uniform concentric circular arrays," *Journal of Electromagnetic Waves and Applications*, Vol. 20, No. 14, 2077–2089, 2006.
4. Abdelaziz, A. A., "Improving the performance of an antenna array by using radar absorbing cover," *Progress In Electromagnetics Research Letters*, Vol. 1, 129–138, 2008.
5. Capineri, L., "Estimation of relative permittivity of shallow soils by using the ground penetrating radar response from different buried targets," *Progress In Electromagnetics Research Letters*, Vol. 2, 63–71, 2008.
6. Landesa, L., et al., "Bias of the maximum likelihood DOA estimation from inaccurate knowledge of the antenna array response," *Journal of Electromagnetic Waves and Applications*, Vol. 21, No. 9, 1205–1217, 2007.
7. Zainud-Deen, S. H., et al., "Direction of arrival and state of polarization estimation using radial basis function neural network (RBFNN)," *Progress In Electromagnetics Research B*, Vol. 2, 137–150, 2008.
8. Xiao, S., et al., "Spatial focusing characteristics of time reversal UWB pulse transmission with different antenna arrays," *Progress In Electromagnetics Research B*, Vol. 2, 223–232, 2008.

9. Fakoukakis, F. E., et al., "Development of an adaptive and a switched beam smart antenna system for wireless communications," *Journal of Electromagnetic Waves and Applications*, Vol. 20, No. 3, 399–408, 2006.
10. Guo, B., Y. Wang, J. Li, P. Stoica, and R. Wu, "Microwave imaging via adaptive beamforming methods for breast cancer detection," *Journal of Electromagnetic Waves and Applications*, Vol. 20, No. 1, 53–63, 2006.
11. Vescovo, R., "Beam scanning with null and excitation constraints for linear arrays of antennas," *Journal of Electromagnetic Waves and Applications*, Vol. 21, No. 2, 267–277, 2007.
12. Kazemi, S., et al., "Performance improvement in amplitude synthesis of unequally spaced array using least mean square method," *Progress In Electromagnetics Research B*, Vol. 1, 135–145, 2008.
13. Seligson, C. D., "Comments on 'High resolution frequency-wavenumber spectrum analysis'," *Proc. of the IEEE*, Vol. 58, 947–949, 1970.
14. Cox, H., "Resolving power and sensitivity to mismatch of optimum array processors," *J. Acoust. Soc. Amer.*, Vol. 54, No. 3, 771–785, 1973.
15. Mouhamadou, M., P. Vaudon, and M. Rammal, "Smart antenna array patterns synthesis: Null steering and multi-user beamforming by phase control," *Progress In Electromagnetics Research*, PIER 60, 95–106, 2006.
16. Liu, Y.-T. and C.-W. Su, "Wideband omnidirectional operation monopole antenna," *Progress In Electromagnetics Research Letters*, Vol. 1, 255–261, 2008.
17. Cox, H., R. M. Zeskind, and M. H. Owen, "Robust adaptive beamforming," *IEEE Trans. Acoust., Speech, Signal Processing*, Vol. 35, No. 10, 1365–1376, 1987.
18. Vorobyov, S. A., A. B. Gershman, and Z. Q. Luo, "Robust adaptive beamforming using worst-case performance optimization: A solution to the signal mismatch problem," *IEEE Trans. Signal Processing*, Vol. 51, No. 2, 313–324, 2003.
19. Li, J., P. Stoica, and Z. Wang, "On robust capon beamforming and diagonal loading," *IEEE Trans. Signal Processing*, Vol. 51, No. 7, 1702–1715, 2003.
20. Lorenz, R. G. and S. P. Boyd, "Robust minimum variance beamforming," *IEEE Trans. Signal Processing*, Vol. 53, No. 5, 1684–1696, 2005.

21. Vorobyov, S. A., Y. Rong, and A. B. Gershman, "Robust adaptive beamforming using probability-constrained optimization," *Proc. IEEE Workshop on Statistical Signal Processing*, 934–939, Bordeaux, France, 2005.
22. Vorobyov, S. A., A. B. Gershman, and Y. Rong, "On the relationship between the worst-case optimization and probability-constrained approaches to Robust adaptive beamforming," *Proc. 32nd IEEE Int. Conference on Acoustics, Speech, and Signal Processing (ICASSP)*, Vol. 2, 977–980, Honolulu, HI, USA, 2007.
23. Reed, I. S., J. D. Mallett, and L. E. Brennan, "Rapid convergence rate in adaptive arrays," *IEEE Trans. Aerospace and Electron. Syst.*, Vol. 10, No. 6, 853–863, 1974.
24. Capon, J., "High resolution frequency-wavenumber spectral analysis," *Proc. of the IEEE*, Vol. 57, No. 8, 1408–1418, 1969.
25. Besson, O. and F. Vincent, "Performance analysis of beamformers using generalized loading of the covariance matrix in the presence of random steering vector errors," *IEEE Trans. Signal Processing*, Vol. 53, No. 2, 452–459, 2005.
26. Proakis, J. G., *Digital Communications*, 4th edition, McGraw-Hill, 2001.
27. Papoulis, A., *Probability, Random Variables, and Stochastic Processes*, 3rd edition, McGraw Hill Company, 1991.
28. Boyd, S. and L. Vandenberghe, *Convex Optimization*, Cambridge university press, Cambridge, 2004.
29. Chang, L. and C. C. Yeh, "Performance of DMI and eigenspace-based beamformers," *IEEE Trans. Antennas Propagat.*, Vol. 40, No. 11, 1336–1347, 1992.